Dust formation in turbulent media

Christiane Helling[1], Marcus Lüttke[1], Erwin Sedlmayr[1], Rupert Klein[2]

Abstract. The present study investigates the role of turbulence in generating an inhomogeneous distribution of solid particles in rarefied gases where colliding gas elements produce acoustic waves with associated temperature, pressure and density enhancements. The dominant physical interactions in the reactive, dust-forming gas flow are estimated and detailed multi-dimensional simulations of compressible fluid-dynamics including dust formation kinetics have been carried out exemplary for physical conditions typical for brown dwarf atmospheres. The dust particle density directly maps the gas density distribution. An inhomogeneous distribution of the dust results. Since the dust formation time scales are considerably smaller than the hydrodynamic time scale, the largest particles are formed at sites of the highest density. Resulting expansion waves cause a decrease of temperature which becomes essential in hot environments.

1. Introduction

Small, solid particles (dust grains) and turbulent motions are phenomena both present in a wide variety of astrophysical objects. For example, the observations of brown dwarfs – very faint and cool stars – strongly indicate both the existence of convective energy transport into the atmosphere ([8]) and the depletion of molecules due to the formation of solid compounds ([11]). The consideration of characteristic scales for brown dwarf atmospheres leads to large Reynolds numbers of $\approx 10^8 \dots 10^{10}$ which also prod to the turbulent character of the gas in such an atmosphere. Convection could provide a mechanism of energy and matter transfer into the atmosphere of a brown dwarf which previously has been depleted by the formation and the gravitational settling of dust grains (Fig. 1).

The progenitor molecules of the dust grain formation already exist in the warm atmospheric regions of $T \approx 2000 \dots 3000\,\mathrm{K}$. As the temperature decreases outwards, more and more complex molecules form and the gas-solid phase transition takes place at lower (threshold) temperatures which are different for each grain compound. The dust grains play an essential role for the thermal balance of the surrounding medium due to their capability to efficiently absorb and scatter the light, thereby improving or worsening the conditions for their own existence.

We present a first study of the micro-physics of a dust forming turbulent medium. We adopt a gas box model with an appropriate scaling according to the

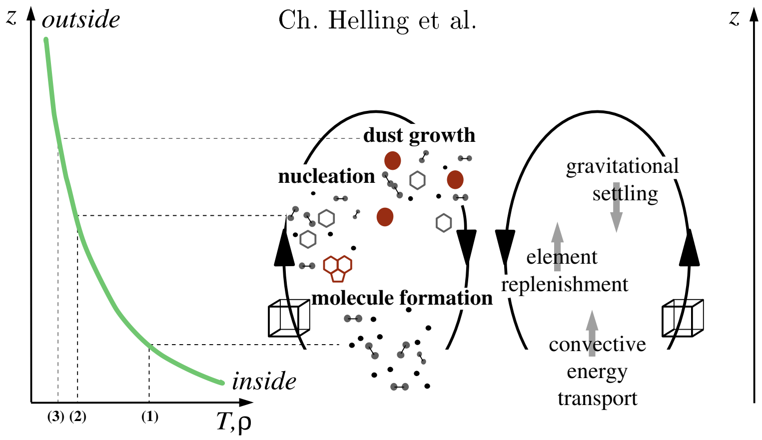

FIGURE 1. Convective energy and momentum transport may cause an element replenishment of condensation species and a non-static situation in the brown dwarf's atmosphere. Dust grains form out of the gas phase from molecules (1) via nucleation (2) and grain growth (3). The gravitational settling of the grains causes the observable depletion of the gas phases.

physical conditions in order to verify two hypotheses for the origin of intermittent dust distributions:

1. *Turbulent momentum exchange* (i.e. colliding gas cells) can improve the conditions for dust formation because
   - the density locally increases in the colliding zones while
   - the gas temperature increase is balanced by fast radiative cooling.
2. Hot and dense gas cells from inside the star cause a *inhomogeneous distribution of condensation species* in the upper atmosphere due to turbulent mixing which is directly mapped by the dust formation.

2. Model problem of a reactive, dust forming gas flow

The physical processes in a reactive, dust forming gas flow, like in a brown dwarf's atmosphere, are described by the following model which contains the description of the hydrodynamics, the thermodynamics, and of the dust complex.

a) HYDRO- AND THERMODYNAMICS:

$$(\rho)_t + \nabla\cdot(\rho\boldsymbol{v}) = 0 \qquad \text{equation of continuity} \qquad (1)$$

$$(\rho\boldsymbol{v})_t + \nabla\cdot(\rho\boldsymbol{v}\circ\boldsymbol{v}) = -\nabla P + \rho\boldsymbol{g} \qquad \text{equation of motion} \qquad (2)$$

$$(\rho e)_t + \nabla\cdot(\boldsymbol{v}[\rho e + P]) = Q_{\rm rad} \qquad \text{energy equation} \qquad (3)$$

$$\rho e = \frac{\rho\boldsymbol{v}^2}{2} + \frac{P}{\gamma-1} - \rho g y \qquad \text{energy density} \qquad (4)$$

$$P = \frac{\rho}{\mu m_{\rm H}} kT \qquad \text{perfect gas law} \qquad (5)$$

$$Q_{\rm rad} = 4\sigma\kappa(T_{\rm RE}^4 - T^4) \qquad \text{net radiative heating rate} \qquad (6)$$

ρ, $\boldsymbol{v}$, P, and e are the state variables density, velocity vector, gas pressure, and total energy of the gas flow. $\boldsymbol{g}$ is the gravitational acceleration pointing towards the stars, $m_{\rm H}$ the mass of the hydrogen atom, and k the Boltzmann constant. T is the gas temperature and $T_{\rm RE}$ the radiative equilibrium temperature. The material quantities entering this model complex are the isentropic exponent γ, the opacity of the medium per mass unit κ, and the mean molecular weigh μ. Additional equations or assumptions are needed to close the system of equations: γ, μ are constant but κ is a result of the dust complex.

b) Dust complex:
The dust complex is described by the momentum method for dust nucleation, growth, evaporation, and chemical sputtering developed by [3] and [4] which has been extended to heterogeneous dust growth by [2]:

$$\rho L_{\rm j} = \int_{V_l}^{\infty} V^{\rm j/3} f(V)\, dV \qquad j^{\rm th} \text{ dust moment} \tag{7}$$

$$(\rho L_0)_t + \nabla\cdot(\boldsymbol{v}\,\rho L_0) = J_* \qquad 0^{\rm th} \text{ moment equation} \tag{8}$$

$$(\rho L_{\rm j})_t + \nabla\cdot(\boldsymbol{v}\,\rho L_{\rm j}) = V_l^{\rm j/3} J_* + \frac{{\rm j}\chi^{\rm net}}{3}\rho L_{\rm j-1} \qquad \text{higher moments} \tag{9}$$

$$\mathrm{j} = \{1,2,3\}$$

The dust moments $L_{\rm j}$ [$\mathrm{cm^j\,g^{-1}}$] are defined as integrals of the grain size distribution function $f(V)$ with V being the grain volume. The source term of Eq. (8), the nucleation rate $J_* = J_*(T, n_{\rm y}(T,\rho,\epsilon_{\rm i}))$, depends on the local thermodynamic conditions (T,ρ) and on the element composition $\epsilon_{\rm i}$ of the gas (i$= 1\ldots N$, N total number of elements). The number density $n_{\rm y}$ of the gaseous species y is calculated assuming chemical equilibrium but may as well result from a detailed network of chemical reactions. J_* is a very strong function of T as can be observed from Fig. 3 (right) where J_* changes by about 40 order of magnitudes at $T \approx 1200$ K (depending on density). Equation (8) yields the number of dust particles formed and the higher order moment equations (Eq. 9) describe the growth and evaporation of existing dust grains, providing e.g. the mean dust volume which enters into the computation of the absorption coefficient κ (see Eqs. 3, 6).

2.1. Dust formation

Brown dwarf atmospheres are composed of a hydrogen-rich gas with an overabundance of oxygen over carbon since almost all carbon is tied up in the CO molecule. As a consequence, oxygen bearing molecules like SiO, VO, MgO, FeO and TiO_2 will be involved in the dust formation and compounds like $Al_6Si_2O_{13}$ or Mg_2SiO_4 may form ([**?**]). Dust formation is treated as a two-step process where at first seed particles condense out of the gas phase (nucleation, Fig. 1) and secondly, surface reactions cause the pre-existing particles to grow (dust growth, Fig. 1). Consequently, two central problems arise: the calculation of the rate of formation of clusters from the gaseous phase and the thermal stability of the grain clusters.

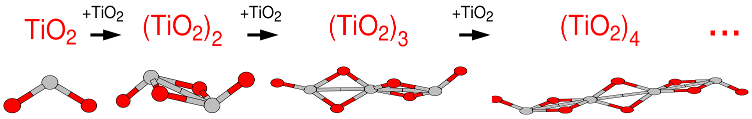

FIGURE 2. Linear reaction chain of homogeneous $(TiO_2)_N$ nucleation. The various structures and thermodynamic potentials of the clusters have been calculated by applying density functional theory by [6].

Dust nucleation: For calculation of the nucleation rate J_*, the *modified classical nucleation theory* relies on the thermodynamic functions of the individual small clusters which are provided by quantum-mechanical (e.g. [9],[1]) or semi-empirical (e.g. [7]) methods. These approaches are presently limited to chemically homogeneous clusters which may form via a linear chain of chemical reactions where one monomer per reaction step is added. A linear growth chain of complex TiO_2-clusters is depicted for the first growth steps in Fig. 2. For determining the nucleation rate, a stationary flux through the cluster space is assumed.
Dust growth: The growth/evaporation process is essentially defined by the addition/ subtraction of growth species to/from the already existing surfaces ([3],[4]). The necessary thermal stability is expressed by the (heterogeneous) net growth velocity $\chi^{\rm net}$ which contains the information of all the dust materials g forming the grain and all the reactions forming the material g. The dust material is thermally stable if $\chi^{\rm net} > 0$, i.e. if for material g the supersaturation ratio $S_{\rm g}(T, n_{\rm y}) \gg 1$.

Figure 3 depicts a stability sequence, i.e. those temperature where $S_{\rm g}(T, n_{\rm y}) = 1$, for various solid compounds g in an oxygen-rich gas like in e.g. brown dwarf atmospheres (for a lower-density-regime see [12]). The compound g is thermally stable below such a curve but evaporates at higher temperatures. Since a typical trajectory crosses the stability sequence from high to low (T, $n_{\rm <H>}$), the compounds become stable one after another. It is remarkable that all materials become stable in a relatively narrow temperature interval which indicates that heterogeneous growth has to be expected. Note the considerable gap between the temperature where $S_{\rm g} = 1$ (Fig. 3, l.h.s.) and the temperature of efficient nucleation (Fig. 3, r.h.s.) e.g. for TiO_2.

2.2. Dominant interactions

These more general considerations are now applied to the physical situation of brown dwarf atmospheres by scaling the model equations (1)–(9) to particular reference values. The discussion of the resulting characteristic numbers provides thereby insight in the dominating interactions between hydrodynamics and dust formation.
Mach number, Froud number: For a typical micro-turbulence velocity[1] v substantiated by interpretations of observations (e.g. [5]) the Mach number $\mathrm{M}^2 = v^2/c_{\rm T}^2$ is approximately 1 with $c_{\rm T} = P^2/\rho^2$ as the isothermal sound velocity. Therefore, we adopt $v_{\rm ref} = c_{\rm T}$ as the reference velocity in the following. A typical

[1]statistical fluctuation

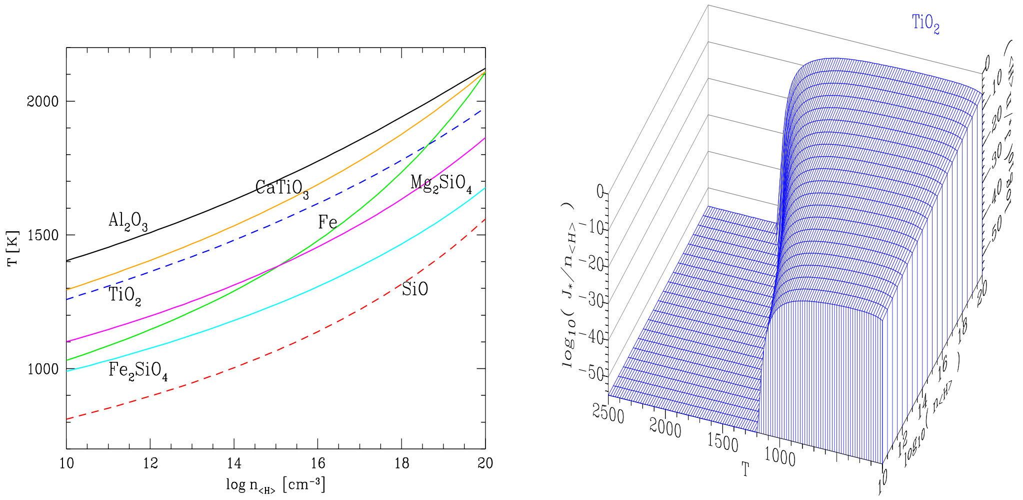

FIGURE 3. Left: Sublimation temperatures ($S_{\rm g}=1$) of various solid compounds g as function of total hydrogen density $n_{\rm <H>}$ in a gas with solar element abundances. Right: Nucleation rate of TiO_2

length scale is the density scale hight in a brown dwarf atmosphere, therefore $l_{\rm ref} = H_\rho = P_{\rm ref}/g_{\rm ref}\rho_{\rm ref}$ and $\mathrm{Fr}^2 = v_{\rm ref}/(g_{\rm ref}t_{\rm ref}) = 1$. Here, $g_{\rm ref}$ denotes the gravitational reference acceleration and $t_{\rm ref} = l_{\rm ref}/v_{\rm ref}$ is the hydrodynamical time scale. Both, M = Fr = 1 indicate the compressibility of the fluid.

Radiation number: In a radiatively influenced environment like a stellar atmosphere it is necessary to add a corresponding source term, the radiative heating rate $Q_{\rm rad}$, in the energy equation (Eq. 3). The scaling of the energy equation results in a characteristic number $\mathrm{Ra} = 4\kappa_{\rm ref}\sigma T_{\rm ref}^4 \cdot t_{\rm ref}/P_{\rm ref}$, the Radiation number, which relates the radiative energy contents and the thermal energy contents of the gas (see Eq. 12). The important quantity in Ra is the absorption coefficient κ which can change by orders of magnitude if dust forms, and consequently $\mathrm{Ra} \approx 10^{-3} \ldots 10$. Therefore, if dust has formed, the Radiation number is large and a singular radiative energy exchange may be present.

Damköhler numbers of Dust Nucleation and Dust Growth: Scaling the dust moment equations provides two dust Damköhler numbers and a characteristic number for the grain size distribution:

1) $\mathrm{Da}^{\rm nuc} = \mathrm{t_{ref}J_{*,ref}}/\rho_{\rm ref}\mathrm{L_{0,ref}}$ is the *Damköhler number of dust nucleation* and relates the number of newly formed dust particles to the number of dust particles formed during the hydrodynamical time $t_{\rm ref}$.

2) $\mathrm{Da}^{\rm gr} = t_{\rm ref}\chi_{\rm ref}/(\frac{4\pi}{3}\langle a\rangle_{\rm ref}^3)^{1/3}$ is the *Damköhler number of dust growth* and relates the grain radius grown during $t_{\rm ref}$ by a growth velocity $\chi_{\rm ref}$ to a typical grain radius $\langle a\rangle_{\rm ref}$.

3) $\mathrm{Se_j} = (a_l/\langle a\rangle_{\rm ref})^{\rm j}$ ($\mathrm{j} = \{1,2,3\}$) is the *Sedlmaÿr number* which characterizes the dust size distribution and relates the minimum particle size a_l in

the definition of the dust moments with a typical grain radius $\langle a\rangle_{\rm ref}$. It depends on the order of the dust moment.

Inserting typical values for $J_{*,\rm ref}$, $L_{0,\rm ref}$, $\chi_{\rm ref}$, $\langle a\rangle_{\rm ref}$, and a_l yields (footnote 3):

$$\mathrm{Da}^{\rm nuc} = 10^6 \qquad \mathrm{Da}^{\rm gr} = 10^4 \qquad \mathrm{Se_j} = 10^{-2}\ldots 1. \tag{10}$$

The time scales on which dust nucleation and growth (e.g. $\tau^{\rm nuc}_{\rm ref} = \rho L_{0,\rm ref}/J_{*,\rm ref}$) take place are much shorter than a typical hydrodynamical time scale and the cooling time scale changes strongly if dust has formed. Therefore, a change of an almost adiabatic to a fast radiatively cooling gas can occur if dust forms. Since dust formation very sensitively depends on temperature, such a behavior causes a strong influence of the hydrodynamics on the dust formation process if e.g. acoustic waves or even shock waves occur.

The analysis of the characteristic numbers shows that the governing equation of our model problem are those of a inviscid (Re$\,\approx 10^8\ldots 10^{10}$), compressible fluid which are coupled to stiff dust moment equations and a singular radiative energy transfer if dust is present. The **dominant interactions** in the model equations (1)–(9) occur in the energy equation (Eq. 12) and in the dust moment equations (Eq. 13, 14) which write in the dimensionless form[2]:

$$\left(\frac{\rho'\boldsymbol{v}'^2}{2} + \frac{P'}{\gamma-1} + \rho' g' z'\right)_{t'} \quad + \quad \nabla'\cdot\left(\boldsymbol{v}'\left[\frac{\rho'\boldsymbol{v}'^2}{2} + \frac{P'}{\gamma-1} + P' + \rho' g' z'\right]\right) \tag{11}$$

$$= \quad \mathbf{Ra}\,\kappa'(1-T'^4) \tag{12}$$

$$(\rho' L'_0)_{t'} + \nabla'\cdot(\boldsymbol{v}'\,\rho' L'_0) \quad = \quad \mathbf{Da^{nuc}}\,J'_* \tag{13}$$

$$(\rho' L'_{\rm j})_{t'} + \nabla'\cdot(\boldsymbol{v}'\,\rho' L'_{\rm j}) \quad = \quad \mathbf{Da^{nuc}}\,\mathbf{Se_j} J'_* + \mathbf{Da^{gr}}\,\frac{{\rm j}\chi^{\rm net\prime}}{3}\rho' L'_{\rm j-1} \tag{14}$$

3. Gas box model of colliding dust-forming gas cells

For testing our hypotheses (Sect. 1), we solve the model equations (1)–(9) in the dimensionless form in a gas box in two space dimensions (x,y) on a multi-dimensional Cartesian grid. The code is based on a Godunov-type compressible Euler solver ([10]) and an operator splitting method is applied for the dust formation and chemistry, the radiative cooling, and the gravity. The grain particles are homogeneous core-mantel grains where the core (seed) consists of TiO_2 and the mantel of SiO. The equilibrium chemistry is solved for approximately 140 molecular species and the elements are conserved. Dust evaporation has not been treated yet.

The initial hydrodynamic values are chosen to initiate an interaction of random gas cells. A matter distribution $\rho'(\boldsymbol{x},0) = p'(\boldsymbol{x},0)$ and some directions of $\boldsymbol{v}$ as

[2]Scaled quantities are indicated by a prime " $'$ ".

depicted in Fig. 4 have been prescribed. The initial state is dust free: $L_j'(\boldsymbol{x},0)=0$. The time and space evolution of these gas cells is studied with special regard to the dust formation in a gas box with reflecting boundaries with a resolution of 90×90 spatial grid points. The gravitational deceleration acts in the negative y-direction.

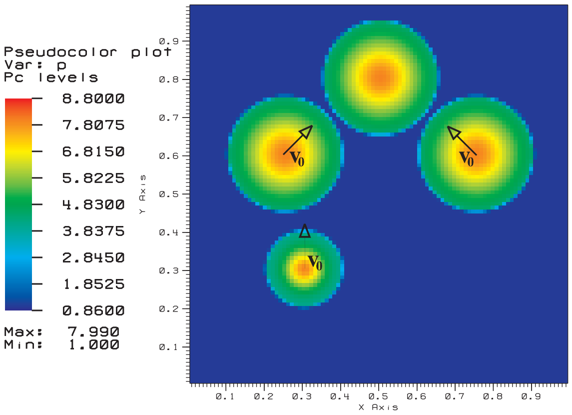

FIGURE 4. Initial conditions: Dust free gas and cells with locally high pressure and density. Arrows indicate the initial velocity direction of the gas cells.

A class of equivalent solutions of the dimensionless model equations, which differ merely by a scale transformation, is determined by the characteristic numbers which correspond to the analysis presented in Sect. 2 ([3]):

$\mathrm{M}=\mathrm{Fr}=1$	$\mathrm{Ra}=10^{-3}$	$\mathrm{Da}^{\mathrm{nuc}}=10^{6}$	$\mathrm{Da}^{\mathrm{gr}}=10^{4}$
$\mathrm{Se}_0=1$	$\mathrm{Se}_1=2\cdot 10^{-1}$	$\mathrm{Se}_2=5\cdot 10^{-2}$	$\mathrm{Se}_3=10^{-2}$

3.1. Results

Figure 5 displays the result of the gas cells time evolution regarding the gas temperature T [K] (l.h.s.) and density ρ [g cm^{-3}] (r.h.s.) in the most evolved situation. Figure 6 depictes as characteristic dust properties the total particle density n_{d} [cm^{-3}] (l.h.s.) and the mean particle radius $\langle a\rangle$ [cm] (r.h.s.) for three instants of time. The last row corresponds to the instant of time depicted in Fig. 5.

While the gas cells expand and the overall density decreases in the gas cells with time, a more and more inhomogeneous temperature and density structure evolves. Warm and dense regions (yellow to red / light to dark) develop due to the collision of the moving gas cells (Fig. 5, l.h.s.) and influence thereby the formation and distribution of dust grains.

As result of the initial condition, the gas cells first travel upward before the gas-dust-mixture falls down due to the gravitational acceleration. Compression

[3] $T_{\mathrm{ref}}=1000\,\mathrm{K}$, $\rho_{\mathrm{ref}}=10^{-5}\ \mathrm{g\,cm^{-3}}$, $t_{\mathrm{ref}}=10\,\mathrm{s}$, $\frac{J_{*,\mathrm{ref}}}{n_{<\mathrm{H}>}}=10^{-2}\ \mathrm{s^{-1}}$, $L_{0,\mathrm{ref}}=10^{11}\ \mathrm{g^{-1}}$, $\langle a\rangle_{\mathrm{ref}}=10^{-6}\,\mathrm{cm}$, $\chi^{\mathrm{net}}_{\mathrm{ref}}=10^{-3}\ \mathrm{cm\,s^{-1}}$

waves develop due to the fast expansion (M=1) of the cells and govern the hydro- and thermodynamics. In the ‘back‘ of the cells an expansion wave causes a drop of T by about 300 K (dark blue / black) which is essential for dust formation in hot environments. The highest temperatures occur in the interaction zones of the compression waves (Fig. 5, l.h.s.) and dust nucleation is prohibited here. Therefore, no TiO_2 is consumed in these hot regions and is therefore available for later seed formation if the gas has been cooled to an appropriate temperature.

The dust particle density $n_{\rm d}$ (Fig. 6, l.h.s.) directly maps the gas density structure: the largest amount of dust particles is present in regions of the highest gas density. This is, however, not true for the mean particle radius $\langle a\rangle$ (Fig. 6., r.h.s.).

The evolution of the mean particle size $\langle a\rangle$ (Fig. 6, r.h.s.) reflects the positive influence of the density on the rate of nucleation: the larger the nucleation rate per mass density, the smaller the final sizes of the dust particles after all condensible material has been used up. Consequently, the mean particle size inside the dense gas cells is smallest whereas it is largest in the thin expansion regions below the upward moving cells where this effect is even amplified and the largest particles are formed.

This effect is superimposed by the time dependence of the growth process which is faster in the more dense regions (Fig. 6, r.h.s., first row) because the surface chemical reactions are more frequent. Consequently, $\langle a\rangle$ increases faster in the dense cells as in the surrounding regions. However, soon all condensible material is consumed inside the cells resulting in no further changes of the mean particle radius with time, which is henceforth only influenced by hydrodynamic motions but not by chemical growth processes. SiO and TiO_2 is then left only outside of the cells where further growth is still possible and consequently, the mean particle radius still increases.

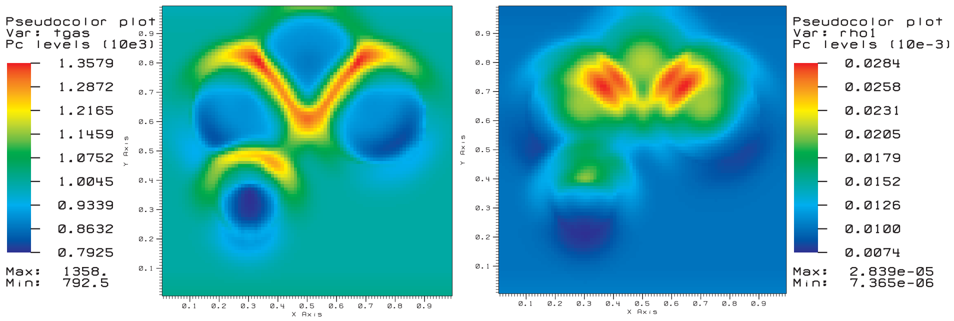

FIGURE 5. The gas temperature T [K] (l.h.s.) and the gas density ρ [g cm^{-3}] (r.h.s.) of colliding gas cells at the most evolved state in a box of the size of $l_{\rm ref} = H_\rho$ in each direction for a chosen set of reference values.

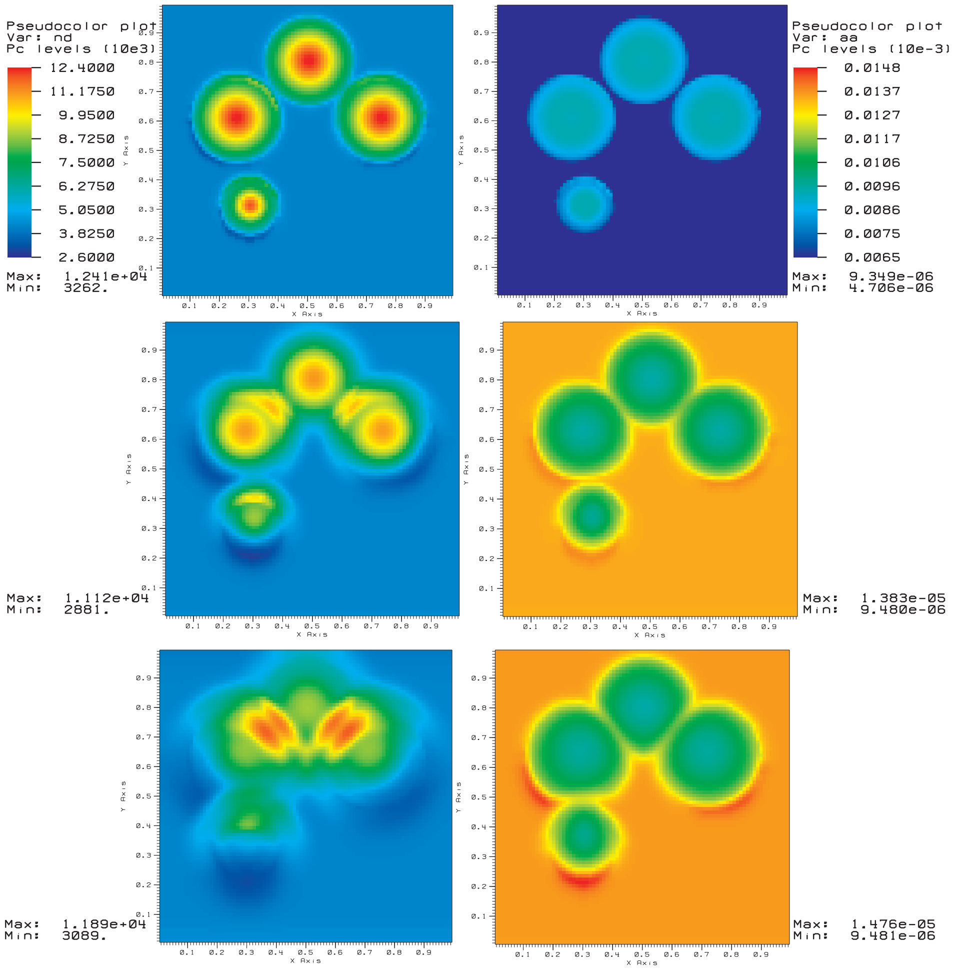

FIGURE 6. Time sequence: The dust particle density $n_{\rm d}$ [cm^{-3}] (l.h.s.) and the mean particle radius $\langle a \rangle$ [cm] (r.h.s) during the gas cells evolution. The first row depicts the least evolved, the third row the most evolved state. All plots are shown in the same interval of the quantities but the maximum and minimum values at the depicted instants of time are given beside.

4. Conclusions & Outlook

Turbulent motion, envisioned as colliding gas cells, can be the cause of an intermittent dust distribution in a brown dwarf's atmosphere since the increase of density in e.g. the colliding zones can improve the conditions for dust growth. Furthermore, the fast adiabatic cooling as a result of the expansion waves can even provide temperatures low enough to initiate dust nucleation in hotter environments than depicted here. In contrast, dust nucleation is inhibited in spots of high temperature in the case of strong compression and unefficient radiative cooling. Since we have solved a system of dimensionless equations, a simple rescaling compatible with the chosen characteristic numbers allows for the application of our results to e.g. other thermodynamic conditions and therby to other regions in brown dwarf atmospheres or other stars. Nevertheless, much work still needs to be done since we know (i) grain mantels have a heterogeneous composition and may change their mineralogical structure during their evolution, (ii) dust and gas receive energy and momentum from inside the star which also allows for a replenishment of the condensation species due to the open inner boundary, (iii) dust and gas may move with different velocities which finally results in a sedimentation process. Furthermore, asymptotic analysis for large Radiative and Damköhler numbers is forseen to provide an independent corroboration of the numerical results and a deeper inside in the dominating interaction which govern the solution of the system of interest.

Acknowledgements We thank M. Oevermann and P. Woitke for careful reading of the manuscript and P. Woitke for providing Fig. 3. H. Schmidt is thanked for providing his hydro-code and for the generous support in setting up the computations. This work was supported by the *DFG* (grants Se 420/19–1, Kl 611/8–1).

References

[1] Chang C., Patzer A. B. C., Sedlmayr E., Sülzle D., 1998, Eur. Phys. J. D 2, 57–62

[2] Dominik C., Sedlmayr E., Gail H.-P., 1993, A&A 277, 578–594

[3] Gail H.-P., Sedlmayr E., 1988, A&A 206, 153–168

[4] Gauger A., Gail H.-P., Sedlmayr E., 1990, A&A 235, 345–361

[5] Hauschildt P., Allard F., Baron E., 1999, ApJ 512, 377–385

[6] Jeong K. S., Chang, Ch., Sedlmayr, E., Sülzle, D., 2000, J. Phys. B 33, 3417–3430

[7] Köhler T. M., Gail H.-P., Sedlmayr E., 1997, A&A 320, 553–567

[8] Oppenheimer B. R., Kulkarni S. R., Matthews K., Nakajima T., 1998, ApJ 502, 932

[9] Patzer A. B. C., Köhler T., Sedlmayr E., 1995, Planet.& Sp.Sci. 43, 1233–1239

[10] Smiljanovski V., Moser V., Klein R., 1997, Combust. Theory Modelling I, 183–215

[11] Tsuji T., Ohnaka K., Aoki W., 1999, A&A 520, L19–L22

[12] Woitke P., 2000, In Diehl R., Hartmann D., *Astronomy with Radioactivities*, 163–174, MPE Report 274

[1] Zentrum für Astronomie & Astrophysik, Technische Universität Berlin, Germany
[2] FB Mathematik & Informatik, Freie Universität Berlin, Germany
E-mail address: chris@astro.physik.tu-berlin.de